# Investigation of the Impact of the Selenization Temperature on Parameters of CIS Thin Films

N. Yeranyan[1], S.Petrosyan[1,2], A. Musayelyan[1], L. Arutiunyan[1], K. Avdjyan[1]

[1]*Institute of Radiophysics and Electronics, NAS RA, Alikhanyan Brs. str.1. 0203, Ashtarak, Armenia*
[2]*Russian-Armenian (Slavonic) University, H. Emin str.123, Yerevan 0051, Armenia*

E-mail: eranyan.narek@gmail.com

Received 30 January 2017

**Abstract.** The CIS thin films were prepared by magnetron sputtering of Cu and In layers on a soda-lime glass substrate from high purity elemental targets, that had been followed by the selenization of thus prepared samples placed in graphite container inside the heated vacuum chamber. This procedure was carried out at various temperatures to determine its impact on the particle size, surface roughness, layer thickness, lattice parameters and the ratio of phases present in the compound. Investigations showed the formation of 3 phases: $CuInSe_2$ with (112) and (220) preferred orientations, $Cu_2Se$ ($Cu_{1.8}Se$ – Berzelianite) and $In_2O_3$ (Indium oxide) without ordered orientations. AFM and XRD analysis were performed. Gaussian and Cauchy (Lorenzian) functions were established as best matched within the created model. It was determined that selenization temperature has a significant influence on the structural and compositional parameters of the CIS thin films. In particular, the crystallite size and the percentage of $CuInSe_2$ phase in the structure increases in case of temperature rise until 450°C.

**Keywords:** CIS thin films, selenization.

## 1. Introduction

For nearly 30 years, copper indium diselenide (CIS) thin films have received considerable attention as the most promising absorber candidates for the large-scale production of low cost thin film photovoltaic solar cells. They are regarded as such because of their high absorption coefficient, suitable band gap, high radiation stability, and the fact that the thickness of the absorption layers can be as little as 1-2 micrometers, which is very important from the viewpoint of precursor material usage [1-6]. The current world record of 22.6% efficiency for such devices has been achieved by Zentrum Sonnenenergie & Wasserstoff Forsch Baden in 2016 [7]. Currently $CuInSe_2$ films can be produced by using various techniques, such as spray pyrolysis method, ink printing method, thermal co-evaporation from Cu, In, and Se elemental sources, molecular beam epitaxy, electrodeposition or a two-step process which consists of DC magnetron sputtering of metallic indium and copper precursors followed by their selenization in Ar + Se atmosphere [8-14]. Among this methods, the last one offers a high level of control over film thickness and deposition sequence, as well as a not overly sophisticated process for manufacturing high-quality CIS thin films .

In this work we had produced CIS thin films by sequential DC magnetron sputtering in an argon atmosphere of Cu and In layers on a soda-lime glass substrate from high purity elemental metallic targets, that had been followed by the selenization of thus prepared samples placed in graphite container inside the heated vacuum chamber. This procedure was carried out at various temperatures. Afterward, we studied the effects of selenization parameters on the particle size, layer thickness, average roughness of the surface, lattice parameters and the ratio of phases present in the compound.

## 2. Experimental procedure

CIS thin films were prepared by a two-step process. In the first step, the Cu and In layers were sputtered on a 1x1 cm square shaped soda-lime glass substrates by DC magnetron sputtering. As the sputtering targets were used In and Cu metallic discs with 200 mm diameter and thickness of 4 mm. Their purity was 99.999%. Targets were positioned at 10 cm distance from the substrate during all the experiments. The base pressure in the chamber was $10^{-2}$ mbar. It increases during the deposition process of metallic layers in the argon atmosphere to $9 \cdot 10^{2}$ mbar and $6 \cdot 10^{2}$ mbar for the Cu and In accordingly. The magnetron was operated in DC mode with working current of 400 mA for the deposition of Cu and 200 mA for In. The duration of the process was 200 and 50 minutes, respectively. The deposition was not a single stage process. First, a layer of copper was deposited on the substrate, then indium layer on the copper. This process was repeated 5 times and the structure with the total thickness of 900 nm had been obtained. For the second step, a special graphite container was made to optimize the selenization process.

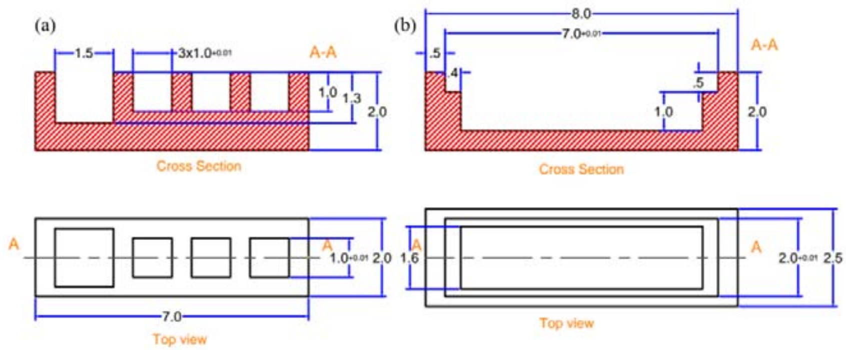


Fig 1. The cross section diagram of graphite container. (a)-the sample holder itself and (b)-its lid.

Granules of pure selenium were put into the larger compartment of the container and the samples with deposited Cu and In layers were inserted in smaller ones. The graphite container was loaded into a quartz tube and evacuated by a mechanical pump to achieve a base pressure of nearly $10^{-2}$ mbar. After that, the quartz tube was put into the heating system. For different batches the treatment was different. Selenization was performed in three steps. At first the samples were kept in 120°C to obtain a good Cu–In alloy where its physical properties become stable. The second step was to heat up to 200°C and keeps them at this temperature for 20 minutes to encourage complete saturation of the alloy precursor with Se [15]. And then depending on a batch for 30 minutes they were kept at 400°C, 450°C, 500°C, 550°C temperature, with the ramp of 40°C per minute for the formation of CIS and the recrystallization process. For all samples, the total selenization time was 60 minutes until the formation of CIS. Properties of obtained $CuInSe_2$ thin films were investigated by grazing incidence X-ray diffraction (XRD) and Atomic Force Microscopy (AFM).

**3. Results and discussion**

In this study, four samples prepared at various selenization temperatures were investigated to establish optimal growth parameters of CIS thin films for further production of CIGS solar cells. The X-ray diffraction patterns with corresponding Rietveld refinements of these samples are presented in Fig. 2 and the Atomic Force Microscopy images of the samples are shown in Fig 3.

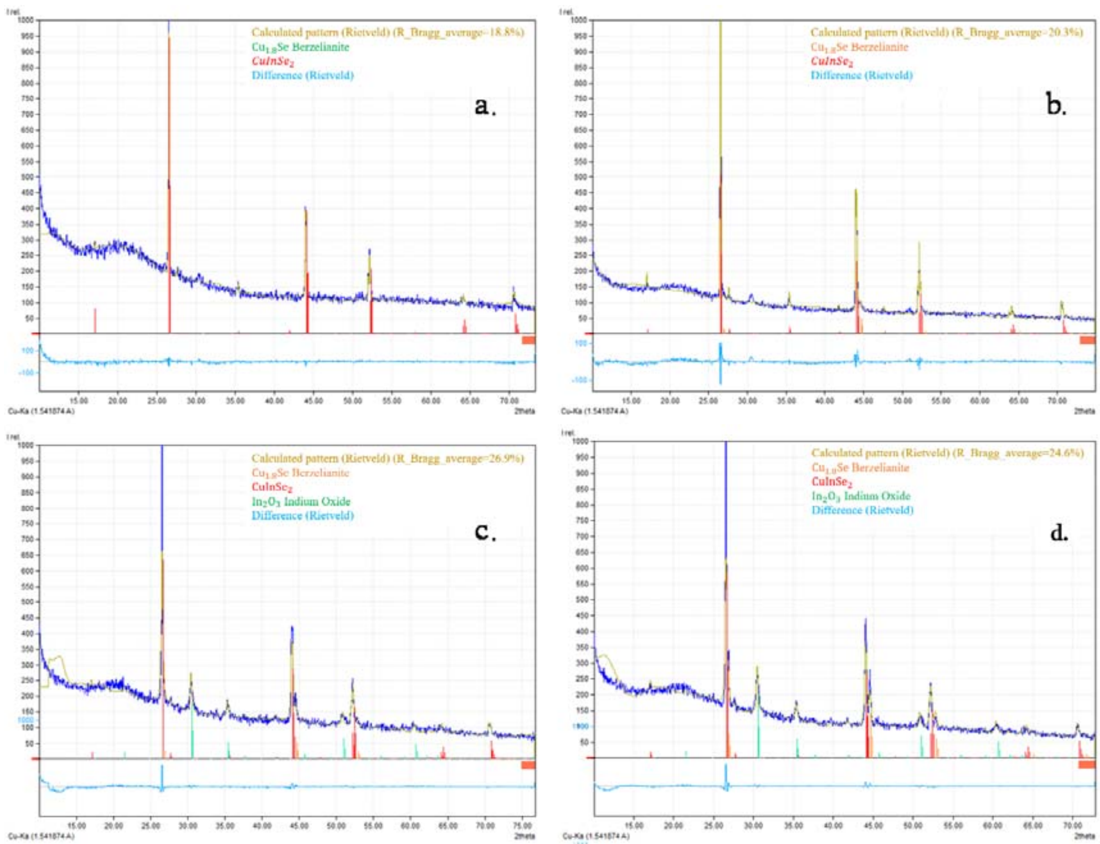


Fig 2. XRD patterns of CIS thin films with different thicknesses prepared at various selenization temperatures: a – 1270nm (selenized at 400$^o$), b – 1315nm (selenized at 450$^o$), c – 1190nm (selenized at 500$^o$), d-820nm (selenized at 550$^o$) with Rietveld analysis.

Most relevant part of data that had been calculated from XRD and AFM analysis are shown in the Table 1. The crystallographic structure and the phases present in the as-prepared CIS thin films were determined by XRD analysis. To find the best fitted profile for our data, Rietveld refinement was done. For that purpose, “Match!” software was used. Two functions were used as profile function: Gaussian and Cauchy (Lorenzian). Refinement also takes into account the shift on 2theta axis, intensity scaling factors of all phases and background parameters. The weighted profile R-factor ($R_{wp}$), which represents discrepancy level of the experimental and computed intensity values ($R_{wp}^2 = \sum_i w_i (y_{c,i} - y_{o,i})^2 / \sum_i w_i (y_{o,i})^2$, where $y_{c,i}$ are the intensity values calculated from the model, $y_{o,i}$ are the observed values, $w_i = 1/\sigma^2[y_{o,i}]$ is weight and $\sigma\,[y_{o,i}]$ is the uncertainty estimate for $y_{o,i}$) [16] was around 20%.

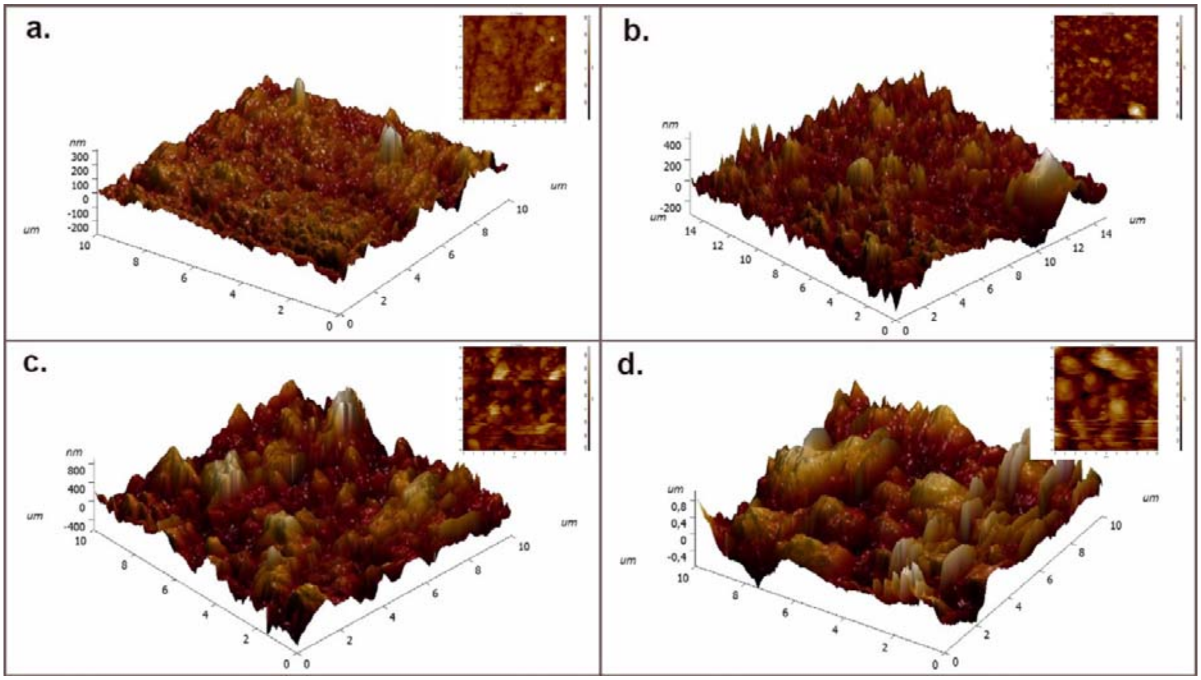


Fig 3. Atomic Force Microscope images of four samples in oblique and plane (inserts) views.

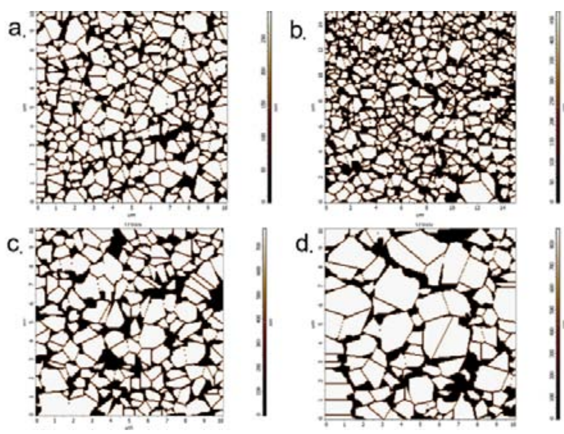


Fig 4. Grain structure of the samples derived from AFM

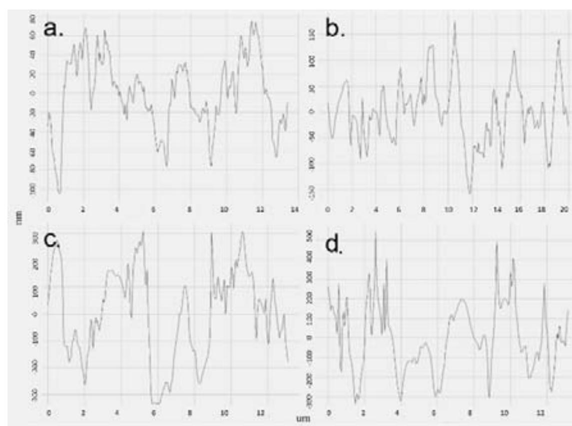


Fig 5. Roughness measurements obtained using AFM line-scan option

On the other hand, the values for "Chi squared" ($\chi^2$) parameter, which is defined as $\left( R_{wp} / R_{\exp} \right)^2$, where $R_{\exp}^2 = N / \sum_i w_i (y_{o,i})^2$ is the expected *R* factor and *N* is a number of data points [16], were close to 1, which means that, eventually, the model fitted into the observed curve.

AFM images of the samples revealed the surface morphology, crystalline sizes and the average roughness $(R_a)$ for each sample. For this purpose images were processed through Gwyddion computer software. The results together with the number of structural, crystallographic and compositional parameters calculated from XRD patterns are summarized in the Table 1.
Obtained layers of $CuInSe_2$ after selenization are polycrystalline. Three phases were observed in the samples structure: $CuInSe_2$, $Cu_{1.8}Se$ (Berzelianite) and $In_2O_3$ (Indium oxide). The formation of above mentioned phases assumed to be represented by the following reactions [17]:

$$2Cu_{11}In_9 + 29Se \Rightarrow 11Cu_2Se + 18InSe \text{ or } 2Cu_{11}In_9 + 20Se \Rightarrow 11Cu_2Se + 9In_2Se,$$

$$\text{then } Cu_2Se + 2InSe + Se \Rightarrow 2CuInSe_2 \text{ or } Cu_2Se + In_2Se \Rightarrow 2CuInSe_2 \text{ respectively,}$$

$$\text{and separately } 4In + 3O_2 \Rightarrow 2In_2O_3.$$

Table 1. Structural and crystallographic properties of DC-plasma sputtered CIS thin films calculated from XRD and AFM analysis.

| Sample | Temp (°C) | Phases | Crystallite size L(nm) | Thickness of the layer (nm) | Lattice parameters | Amount (%) | Density (g/cm$^3$) |
|---|---|---|---|---|---|---|---|
| **a** | 400 | $CuInSe_2$ | 321 | 1270±169 | Tetragonal a = 5.7876 c = 11.604 | 87.3 | 5.69 |
| | | $Cu_2Se$ | 241 | | Cubic a = 5.7762 | 12.7 | 6.756 |
| **b** | 450 | $CuInSe_2$ | 446 | 1315±213 | Tetragonal a = 5.7877 c = 11.6274 | 96.6 | 5.668 |
| | | $In_2O_3$ | 140 | | Cubic a = 10 | 3.4 | 7.075 |
| **c** | 500 | $CuInSe_2$ | 400 | 1230±227 | Tetragonal a = 5.7815 c = 11.616 | 43.6 | 5.692 |
| | | $Cu_2Se$ | 129 | | Cubic a = 5.729 | 36.9 | 6.83 |
| | | $In_2O_3$ | 211 | | Cubic a = 10.117 | 19.6 | 7.123 |
| **d** | 550 | $CuInSe_2$ | 361 | 820±211 | Tetragonal a= 5.7815 c= 11.6159 | 58.5 | 5.746 |
| | | $In_2O_3$ | 220 | | Cubic a = 10.117 | 14.5 | 7.123 |
| | | $Cu_2Se$ | 296 | | Cubic a= 5.729 | 27 | 6.823 |

As it is mentioned in the [18], during selenization of Cu-rich layers, formation of $Cu_xSe$ secondary phase is expected and $CuInSe_2$ phase has a structure of chalcopyrite. Increase of intensity from the reflection of $Cu_xSe$ phase can be noticed in Fig. 6 (phases marked with red color). These secondary phases, unfortunately, can reduce the efficiency of CIS based solar cells, but the composition can be improved by the etching of the samples [19].

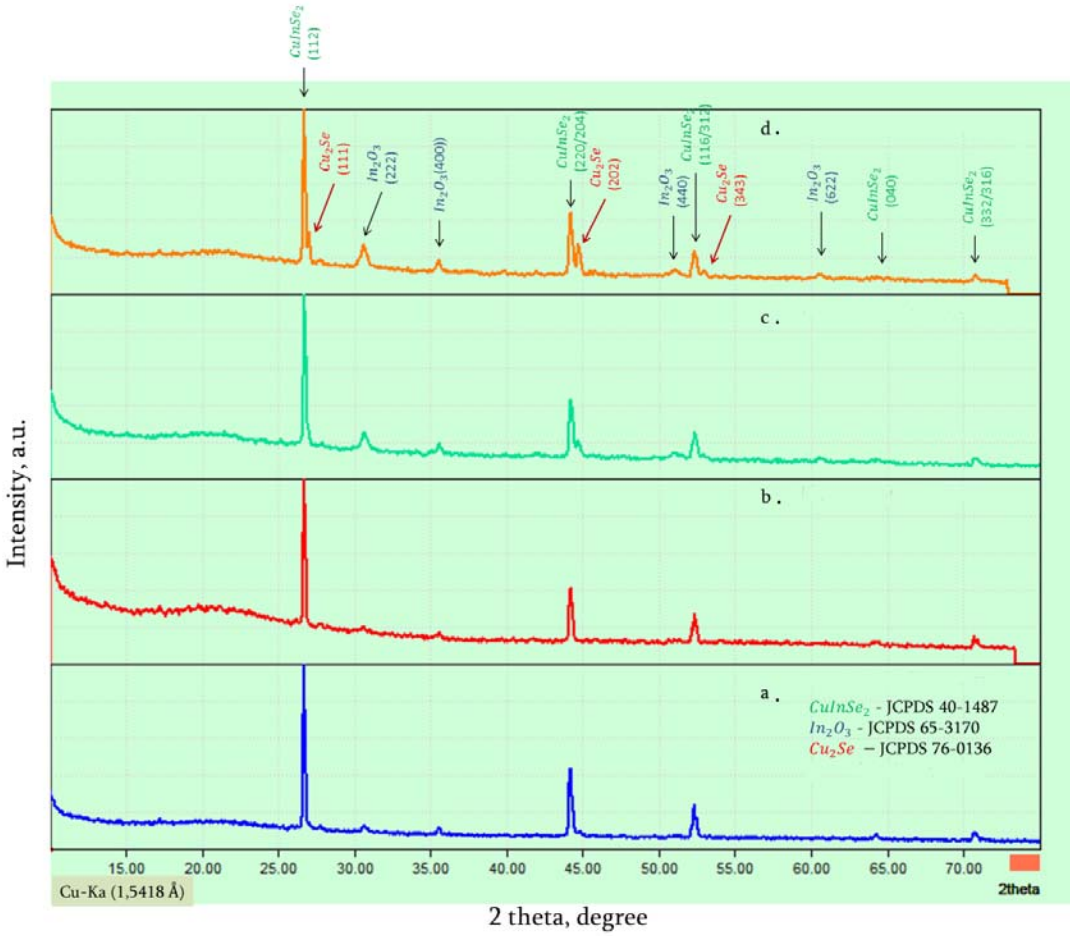


Fig 6. XRD patterns of CIS thin films selenized at different temperatures.

The average crystallite size of the desired $CuInSe_2$ phase increased with the increase of selenization temperature from $400^\circ C$ to $450^\circ C$, but in case of $500^\circ C$ percentage of $CuInSe_2$ starts to decreas along with the decrease in the crystalline size. Both of those values go down with the further increase of the selenization temperature. The thickness of the structure also decreases at higher temperatures due to the evaporation of the materials. Starting from $450^\circ C$ the presence of Indium oxide also was observed, which becomes more significant with further increase of the selenization temperature resulting in the degradation of parameters of the CIS thin films. As it can be seen from AFM images, the surface roughness is lowest for the sample (a) which was selenized at $400^\circ C$ and it increases with the rise of temperature. Smooth films could lower the number of interfacial states between the absorber layer and the window layer in the solar cell, thereby lowering the dark current, which is essential for fabrication of high-quality solar cells [20].

The lattice parameters measured from XRD data for all of the investigated samples are also presented in the table. Lattice constants for $CuInSe_2$ phases were $a$ = 5.784±0.003 Å, $c$ = 11.615±0.01 Å and $c/a$ = 2.008, which is in good agreement with known single crystal data [21].

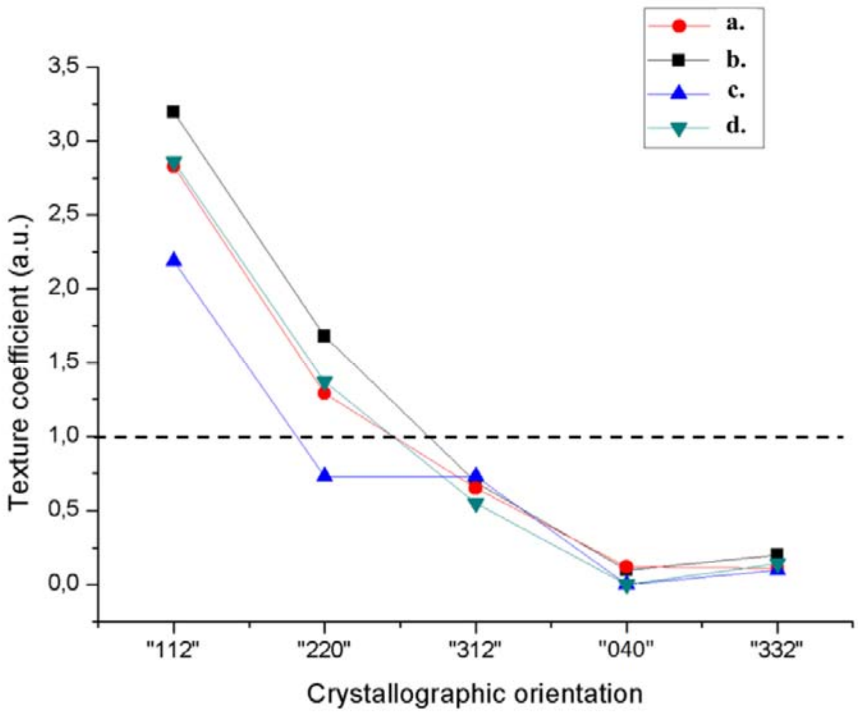


Fig 7. Calculated texture coefficients of the (112), (220), (312), (400) and (332) reflections of the CuInSe2 films.

Additionally, to investigate the preferred orientation of $CuInSe_2$ layers, texture coefficients (*TC*) of given (*hkl*) planes were calculated by the following equation [22]

$$TC(hkl) = \frac{\dfrac{I_{nw}(hkl)}{I_0(hkl)}}{\dfrac{1}{N}\sum_{i=1}^{N}\dfrac{I_{nw}(hkl)}{I_0(hkl)}}$$

where $I_{nw}(hkl)$ and $I_o(hkl)$ are the measured and standard integrated intensities for (hkl) reflection, respectively, and *N* is the number of peaks observed (in our study *N* = 5). The calculated *TC*s are shown in Figure 7. $CuInSe_2$ (112)-oriented grains are clearly textured, since TC was more than 2 for all observed samples (whereas $TC > 1$ indicates preferential orientation). $TC > 1$ also for (220) orientation, except the sample selenized at $450\,^{\circ}C$ which as had been noted possesses biggest crystalline size value and highest percentage of $CuInSe_2$ phase. All the remaining *TC*s are less than one. Thus, XRD patterns of the sputtered and annealed CIS films under Se-containing atmosphere at different temperature revealed a basic chalcopyrite crystalline structure, do not exhibit a clear texture, but show a preferred orientations of (112) and (220)/(204) at 2θ= $26.63^0$ and $44.47^0$, respectively, according to JCPDS card no. 40-1487.

**4. Conclusions**

Polycrystalline $CuInSe_2$ thin films were produced via magnetron sputtering of Cu and In fallowed by their selenization inside graphite container in the heated quartz vacuum tube at 4 different temperatures. The XRD results indicate the formation of 3 phases: $CuInSe_2$ with (112) and (220) preferred orientations, $Cu_2Se$ ($Cu_{1.8}Se$ – Berzelianite) and $In_2O_3$ (Indium oxide) without ordered orientations. XRD and AFM analysis, including Rietveld (for phase identification from powder diffraction data) had shown the average roughness of the structures surface, its crystalline size, percentage of $CuInSe_2$ phase and the thickness of CIS layer. Gaussian and Cauchy (Lorenzian) functions were established as best matched within the created model. It was determined, that selenization temperature has a significant influence on the structural and compositional parameters of the CIS thin films. In particular, an increase of the temperature until $450^\circ C$ provides an increase of the average crystallite size, with the increase of the percentage of $CuInSe_2$ phase in structure. Higher and lower temperatures are causing decrease of these parameters. Moreover, rising temperature above certain degree will damage the structure. The percentage of $CuInSe_2$ phase also will continue to decrease at higher temperatures and $Cu_2Se$ secondary phases became significant.

## Acknowledgments

The authors gratefully acknowledge financial support from “Barepasht Serund” Foundation and RA State Committee of Science under the Grant N15Ap 2b011. Also, the authors would like to thank Dr. Emma Arakelova and Susanna Grigorian for the help in XRD measurements.

**References**

1. W.N. Shafarman, L. Stolt, Handbook of Photovoltaic Science and Engineering, John Wiley & Sons Ltd. (2003) 567.
2. A. Jager-Waldau, Solar Energy Materials and Solar Cells **95**, no. 6 (2011) 1509–1517.
3. S. Niki, M. Contreras, I. Repins et al., Progress in Photovoltaics, **18**, no. 6 (2010) 453–466.
4. O. Lundberg, J. Lu, A. Rockett, M. Edoff, L. Stolt, Journal of Physics and Chemistry of Solids **64**, no. 9-10 (2003) 1499–1504.
5. U. Rau, H. W. Schock, Solar Cells: Materials, Manufacture and Operation, T. Markvart and L. Castaner, Eds., (Elsevier, Oxford, UK, 2005) 303–349.
6. J. R. Tuttle, M. Contreras, A. Tennant, D. Albin, R. Noufi, Proceedings of the 23rd IEEE Photovoltaic Specialists Conference, Louisville, Ky, USA, (1993) 415–421.
7. P. Jackson, R. Wuerz, D. Hariskos, E. Lotter, W. Witte, M. Powalla, Phys. Status Solidi RRL **10**: (2016) 583–586.
8. Sho Shirakata et al, Jpn. J. Appl. Phys. **38** (1999) 4997.
9. V.K. Kapur, A. Bansal, P. Le, O.I. Asensio, Thin Solid Films **431-432** (2003) 53-57.
10. K. Ramanathan, M.A. Contreras, C.L. Perkins, S. Asher, F.S. Hasoon, J. Keane, D. Young, M. Romero, W. Metzger, R. Noufi, J. Ward, A. Duda, Prog. Photovolt: Res. Appl. **11**: (2003) 225–230.
11. I. Repins, M A. Contreras, B. Egaas, C. DeHart, J. Scharf, C.L. Perkins, B. To, R. Noufi, Prog. Photovolt: Res. Appl. **16**: (2008) 235–239.
12. T. Nakada, F. Keisuke, K. Akio, IEEE Transactions on electron devices **46** (10) (1999) 2093-2097.
13. D. Lincot, J.F. Guillemoles, S. Taunier, D. Guimard, J. Sicx-Kurdi, A. Chaumont, N. Bodereau, Solar Energy **77**(6) (2004) 725-737.
14. Pan Tao Ti Hsueh Pao, Chinese Journal of Semiconductors 25(6) (2004) 741-744.
15. T. Nakano, T. Suzuki, N. Ohnuki, S. Baba, Thin Solid Films **344** (1) (1998) 192-195.
16. R.A. Young, The Rietveld Method, edited by R.A. Young (Oxford University Press, Oxford, 1993) 1-38.
17. S. Verma, N. Orbey, R. Birkmire, T. Freser Russel, Progress in Photovoltaics: Research and Applications **4**, (1996) 341-353.
18. Ye.P. Zaretskaya,V.F. Gremenyuk et al., Zhurnal Tekhnicheskoi Fiziki **70** (10) (2000) 141-143 (in Russian).
19. J.H. Schon, V. Alberts, E. Bucher, Thin Solid Films **301** (1997) 115-121.
20. A.M. Hermann, M. Mansour, V. Badri, et.al, Thin Sold Films **361-362** (2000) 74-78.
21. J. Binsma, L.J. Giling and J. Bloem, J. Cryst. Growth, **50** (1980) 429.
22. G.B. Harris, X. Quantitative measurement of preferred orientation in rolled uranium bars, London, Edinburgh, Dublin Phil. Mag. J. Sci. **43** (2009) 113-123.